
Figures and figure supplements

Integrated sensing of host stresses by inhibition of a cytoplasmic two-component system controls *M. tuberculosis* acute lung infection

John A Buglino et al

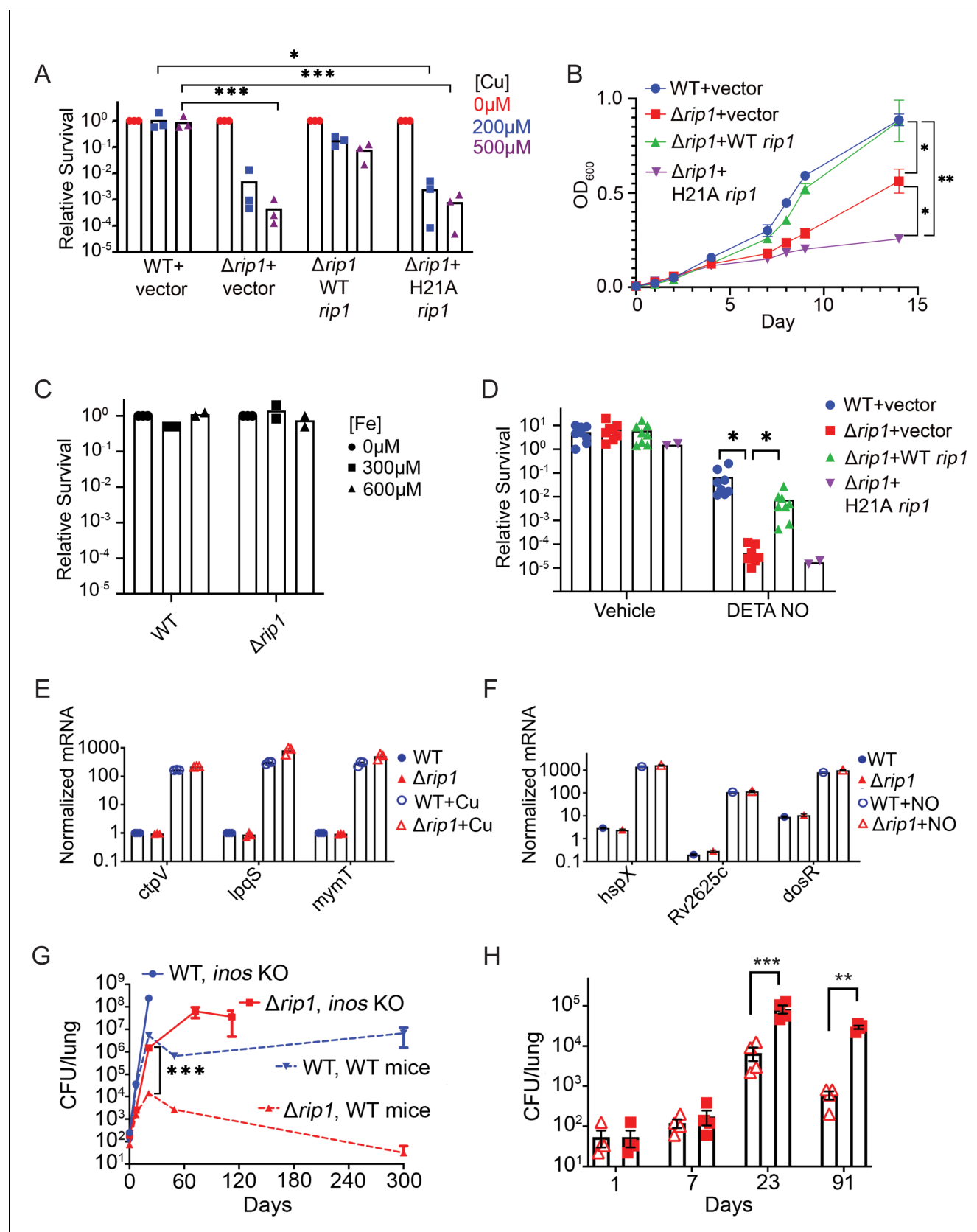


Figure 1. The Rip1 protease controls copper and nitric oxide resistance. (A) The Rip1 pathway confers resistance to copper. Bacterial colony-forming units (CFUs) of the indicated strains grown on agar plates supplemented with 200 or 500 μ M copper sulfate. Relative survival is normalized to untreated

Figure 1 continued on next page

Figure 1 continued

controls, which are set at $10^0 = 1$. Each value is the average of technical duplicate measurements for $n = 3$ biological replicates. Statistical analysis by two-way ANOVA with Tukey's multi-comparison correction * $p < 0.01$ WT + vector 200 μM vs. Δrip1 + H21A *rip1*; *** $p < 0.001$ WT + vector 500 μM vs. Δrip1 + vector; WT + vector 500 μM vs. Δrip1 + H21A *rip1*. (B) The Rip1 pathway confers resistance to zinc. Growth (OD_{600}) of the indicated strains in liquid culture supplemented with 100 μM zinc sulfate. Data plotted is SEM of $n = 3$ biological replicates. Statistical analysis by ordinary one-way ANOVA with Tukey's multi-comparison correction. * $p < 0.05$, ** $p < 0.01$; day 14 WT + vector vs. Δrip1 + vector $p = 0.027$; day 14 Δrip1 + vector vs. Δrip1 + H21A *rip1* $p = 0.032$; day 14 WT + vector vs. Δrip1 + H21A *rip1* $p = 0.002$. (C) The Rip1 pathway does not control iron sensitivity. Growth on agar plates supplemented with 300 or 600 μM iron chloride normalized to untreated controls as in (A). Each value is the average of technical duplicate measurements for $n = 2$ biological replicates. (D) The Rip1 pathway confers resistance to nitric oxide. CFU counts of the indicated strains post treatment with vehicle or 200 μM diethylenetriamine nitric oxide adduct (DETA-NO) for 3 days. Relative survival = CFU day 3 post treatment/CFU at day 0 for each condition $n = 8$ biological replicates for WT + vector, Δrip1 + vector, and Δrip1 + WT *rip1*, and $n = 2$ for Δrip1 + H21A *rip1*. Statistical analysis by unpaired t-test. * $p < 0.05$; DETA-NO WT + vector vs. Δrip1 + vector $p = 0.041$; DETA-NO Δrip1 + vector vs. Δrip1 + WT *rip1* $p = 0.031$. (E) Loss of Rip1 does not affect Cu-induced transcription. RT-qPCR quantitation of known copper-regulated transcripts *ctpV*, *lpqS*, and *mymT* between WT (blue) and Δrip1 (red) cells in resting (filled symbols) or 200 μM copper sulfate (open symbols) conditions for 2 hr. Values are normalized to *sigA* transcript levels. Values represent average of three technical replicate measurements of three biological replicates. (F) Loss of Rip1 does not affect nitric oxide-regulated gene expression through DosR. RT-qPCR comparison of nitric oxide-induced, DosR-regulated transcripts *hspX*, *rv2625c*, and *dosR* between WT and Δrip1 cells following 3 hr of treatment with vehicle (filled symbols) or 200 μM DETA-NO (empty symbols). Values are normalized to *sigA* transcript levels. Mean of biological triplicates reported. (G) NO mediates attenuation of *M. tuberculosis* Δrip1 in mouse lung infection. Bacterial burden (CFU) in lungs of C57bl/6 (broken lines), and age-matched *Nos2*^{-/-} (solid lines) mice infected with WT *M. tuberculosis* (blue) or *M. tuberculosis* Δrip1 (red) at the indicated times (days) post infection. Data plotted is mean and SD of $n = 4$ biological replicates. *** $p = 0.0003$ by unpaired t-test at 21-day time point for Δrip1 in WT vs. *Nos2*^{-/-}. (H) Repeat experiment as in (G), but with lower initial inoculum of Δrip1 *M. tuberculosis* in WT (open triangles) and *Nos2*^{-/-} (closed squares) mice. For all strains/host day 1 $n = 3$ biological replicates; $n = 4$ biological replicates for all other time points. Statistical significance by unpaired t-test analysis is represented as * $p < 0.05$, ** $p < 0.01$, *** $p < 0.001$.

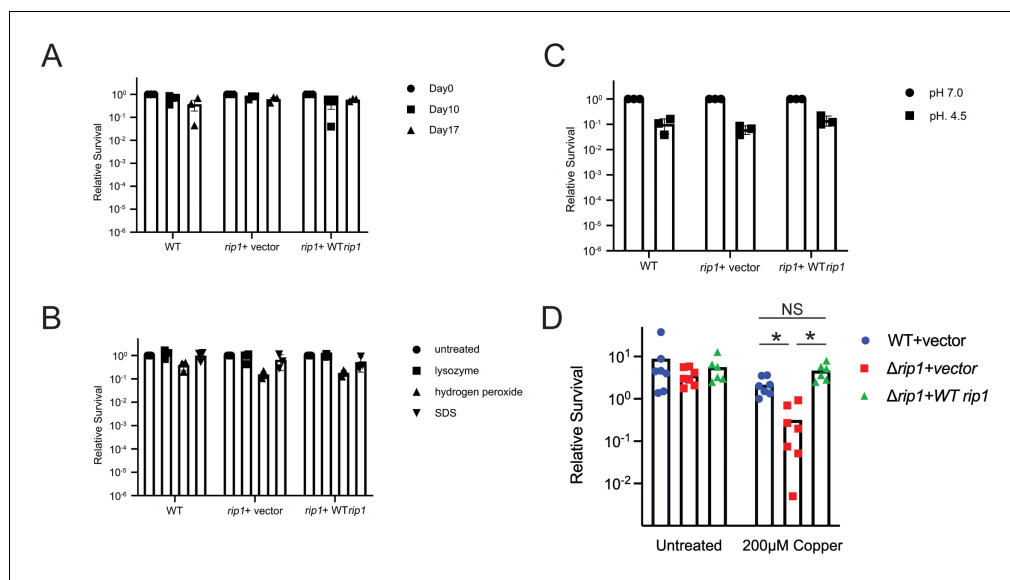


Figure 1—figure supplement 1. Rip1 does not defend against starvation, oxidative stress, detergent, or acid. (A) Phosphate buffered saline (PBS) starvation sensitivity assay. Colony-forming units (CFUs) of the indicated strains were determined at the indicated time points post inoculation into standing flask containing PBS at a seeding density of 0.1 OD₆₀₀. Relative survival = CFU Day X post inoculation/CFU at D0. n = 3 biological replicates. (B) Lysozyme, hydrogen peroxide, and sodium dodecyl sulfate (SDS) sensitivity assay. CFUs of the indicated strains were determined after treatment with 2.5 mg/mL lysozyme, 10 mM hydrogen peroxide, 0.05% SDS for 3 hr. Relative survival = CFU treatment/CFU matched untreated control. n = 3 biological replicates. (C) pH 4.5 survival assay. CFU of the indicated strains was determined after 7 days of incubation in 7H9 ADS media at the indicated pH. Relative survival = CFU pH 4.5/CFU pH 7.0. n = 3 biological replicates. (D) Loss of Rip1 confers sensitivity to Cu in liquid culture. The indicated strains were grown with or without 200 μ M CuSO₄ for 3 days and bacterial survival quantitated by culturing on agar media without copper. n = 7 biological replicates for WT + vector, Δ *rip1* + vector; n = 6 biological replicates for Δ *rip1* + WT *rip1*. *p<0.01 by Welch's t-test.

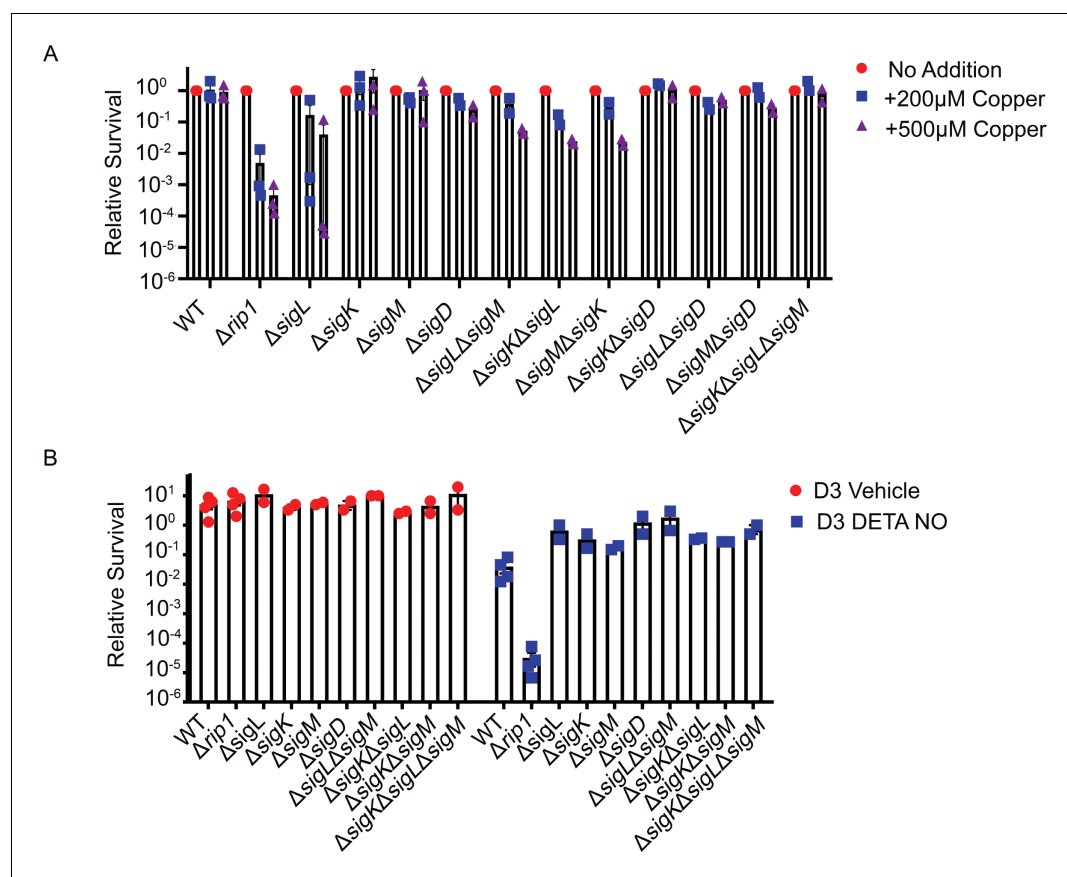


Figure 1—figure supplement 2. Rip1-controlled sigma factor pathways do not contribute to Cu or NO resistance. (A) Agar plate copper sensitivity assay. Colony-forming unit (CFU) of the indicated strains grown on agar plates supplemented with 200 or 500 μ M copper sulfate normalized to untreated controls. Relative survival = CFU treatment/CFU untreated (No Addition). For WT and $\Delta rip1$, each value is the average of technical duplicate measurements for $n = 3$ biological replicates. Values for all other strains are the average of technical duplicates measured for $n = 2$ biological replicates. (B) Nitric oxide sensitivity assay. CFU counts of the indicated strains post treatment with vehicle or 200 μ M diethylenetriamine nitric oxide adduct (DETA-NO) for 3 days. Relative survival = CFU day 3 post treatment/CFU at day 0 for each condition. $n = 4$ biological replicates for WT and $\Delta rip1$. $n = 2$ biological replicates for all other strains.

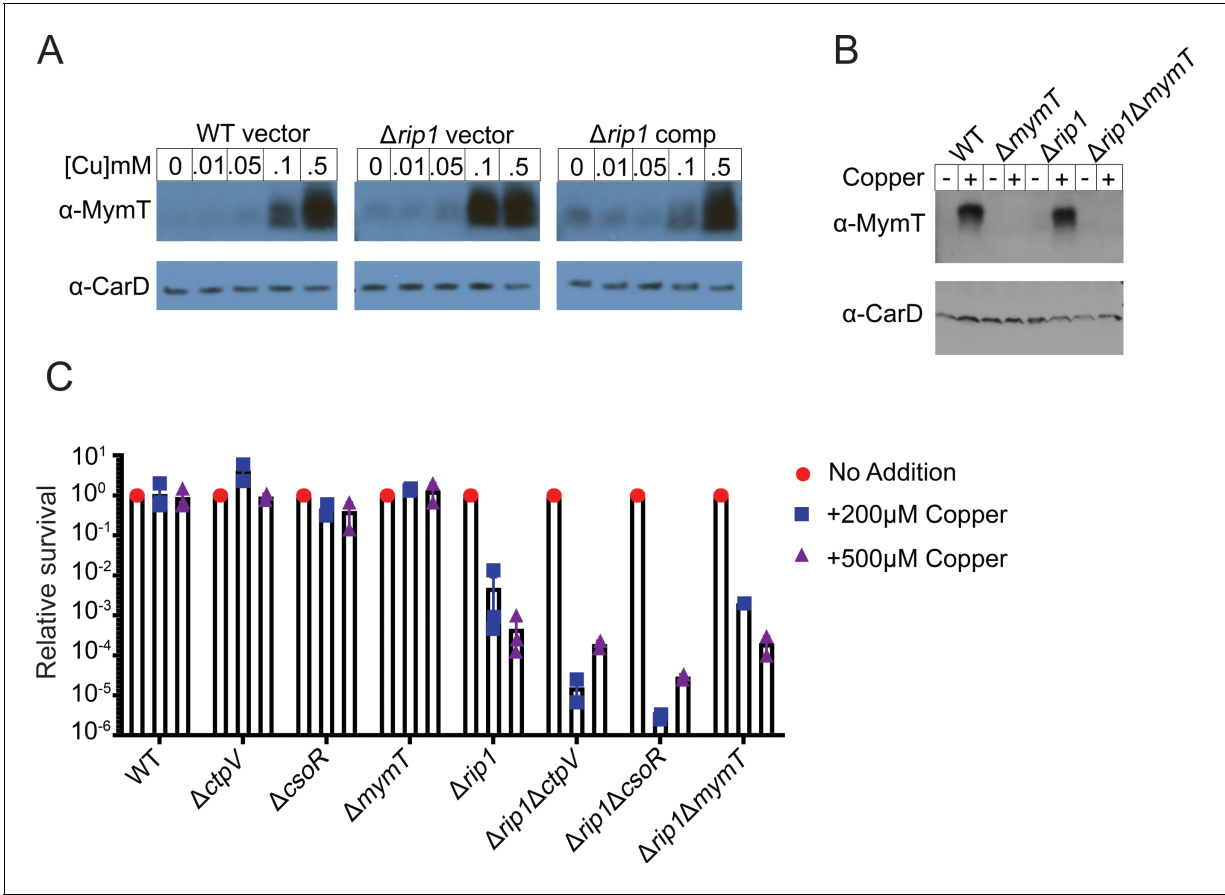


Figure 1—figure supplement 3. Rip1 copper sensitivity is not through known Cu resistance pathways. (A) Rip1 does not control Cu-induced transcription through RicR. Lysates generated from the indicated strains, treated for 2 hr with the indicated concentrations of copper sulfate, were separated by SDS-PAGE and probed with anti-MymT rabbit polyclonal sera (upper panel). Blots were re-probed with rabbit polyclonal sera against CarD (lower panel) to determine relative loading. (B) Immunoblot confirmation of MymT deletion. Lysates generated from the indicated strains treated for 2 hr with 5 mM copper sulfate (+) or without addition of excess copper (-) were separated and probed as described in (A). (C) Rip1 copper sensitivity is independent of CtpV, CsoR, or MymT. Bacterial survival of the indicated strains grown on agar plates supplemented with 200 or 500 μ M copper sulfate normalized to untreated controls. Relative survival = CFU treatment/CFU untreated (No Addition). For WT and $\Delta rip1$, each value is the average of technical duplicate measurements for $n = 3$ biological replicates. Values for all other strains are the average of technical duplicates measured for $n = 2$ biological replicates.

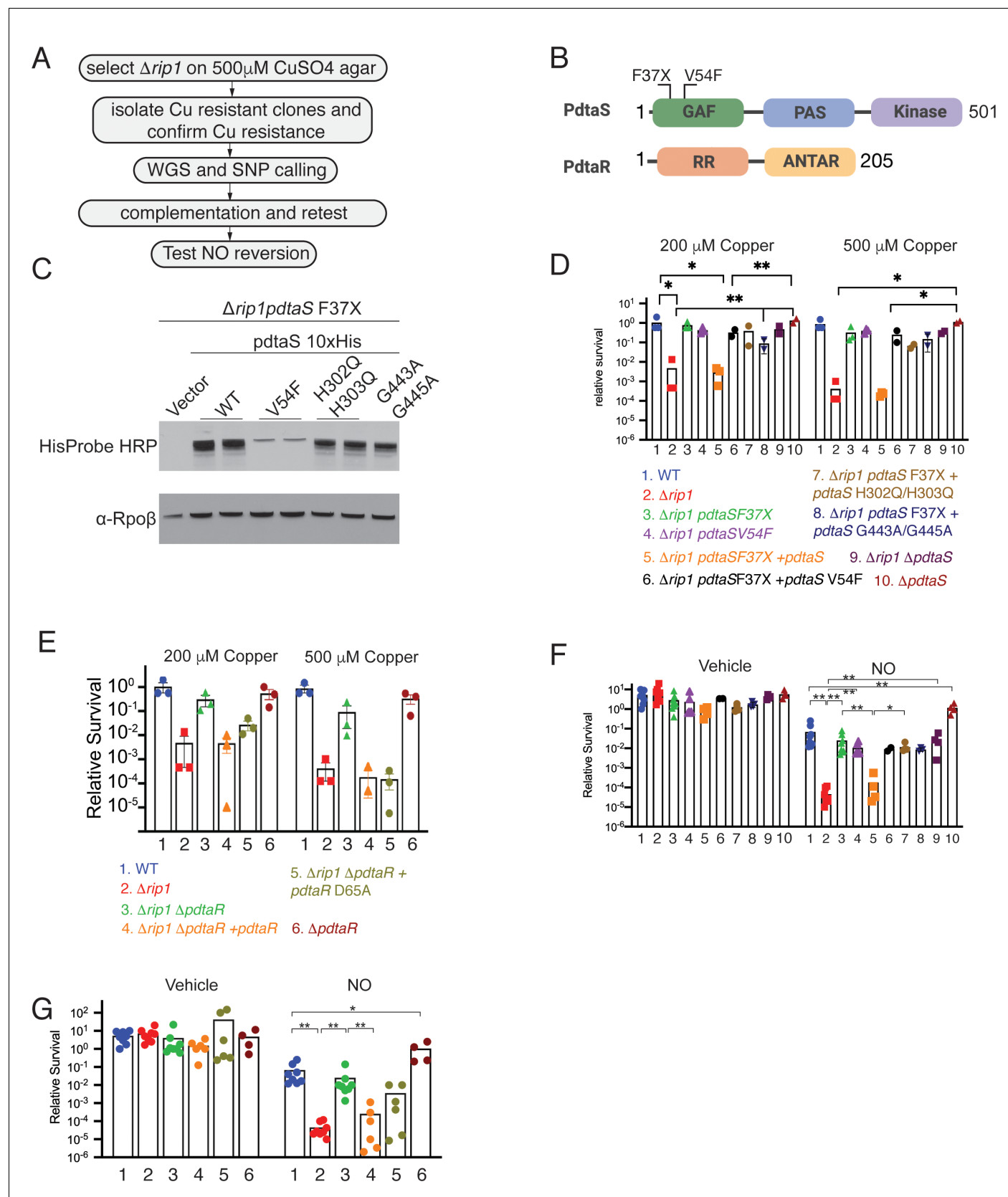


Figure 2. The PdtA/PdtR two-component system controls copper and NO resistance downstream of Rip1. **(A)** Flow chart of a genetic suppressor screen to isolate reversion mutations of the Rip1 Cu sensitivity and testing their reversion of NO sensitivity. WGS: whole genome sequencing; Figure 2 continued on next page

Figure 2 continued

SNP: single nucleotide polymorphism. (B) Domain structure of PdtA with GAF, PAS, and kinase domains. Identified suppressor mutations of PdtA are shown in the N-terminal GAF domain. The reported phosphorylation target of PdtA is the PdtR response regulator (RR), which contains a C-terminal ANTAR RNA binding domain. (C) Protein levels of the indicated alleles of *pdtA* reintroduced into the $\Delta rip1$ *pdtA* F37X background as C-terminal 10X His fusion proteins with RpoB levels as a loading control. For WT, V54F, and H302Q/H303Q, two independent strains are shown, whereas for vector and G443A/G445A, one strain is shown. (D) Loss of *pdtA* suppresses copper sensitivity of $\Delta rip1$. Relative survival of the indicated strains grown on agar plates supplemented with 200 or 500 μ M copper sulfate normalized as in **Figure 1**. H302Q/H303Q and G443A/G445A are kinase dead alleles. Each value is the average of technical duplicate measurements for $n = 3$ biological replicates. Statistical analysis by two-way ANOVA with Tukey's multiple-comparison correction. (E) Loss of *pdtR* suppresses copper sensitivity of $\Delta rip1$. Cu sensitivity assay as noted in (D). PdtR D65A lacks the receiver aspartate for PdtA phosphorylation. Each value is the average of technical duplicate measurements for $n = 3$ biological replicates. (F) Loss of *pdtA* suppresses NO sensitivity of $\Delta rip1$. Colony-forming unit (CFU) counts of the indicated strains post treatment with vehicle or 200 μ M diethylenetriamine nitric oxide (DETA-NO) for 3 days. Color coding of strain genotypes is the same as in (D). $n = 8$ biological replicates for WT, $\Delta rip1$, $\Delta rip1$ *pdtA* F37X; $n = 6$ biological replicates for $\Delta rip1$ *pdtA* V54F; $n = 4$ biological replicates for $\Delta rip1$ *pdtA* F37X + *pdtA*, $\Delta rip1$ *pdtA* F37X + *pdtA* H302Q/H303Q, $\Delta rip1$ Δ *pdtA*, Δ *pdtA*; $n = 3$ biological replicates for $\Delta rip1$ *pdtA* F37X + *pdtA* G443A/G445A; $n = 2$ for $\Delta rip1$ *pdtA* F37X + *pdtA* V54F. Statistical analysis by Mann–Whitney test. (G) Loss of *pdtR* suppresses NO sensitivity of $\Delta rip1$. CFU counts of the indicated strains post treatment with vehicle or 200 μ M DETA-NO for 3 days. Color coding of strain genotype is the same as in (E). $n = 8$ biological replicates for WT, $\Delta rip1$, $\Delta rip1$ Δ *pdtR*; $n = 6$ biological replicates for $\Delta rip1$ Δ *pdtR* + *pdtR* and $\Delta rip1$ Δ *pdtR* + *pdtR* D65A; $n = 4$ biological replicates for Δ *pdtR*. Statistical analysis by Mann–Whitney test. For all panels, statistical significance is represented as * $p < 0.05$, ** $p < 0.01$, *** $p < 0.001$.

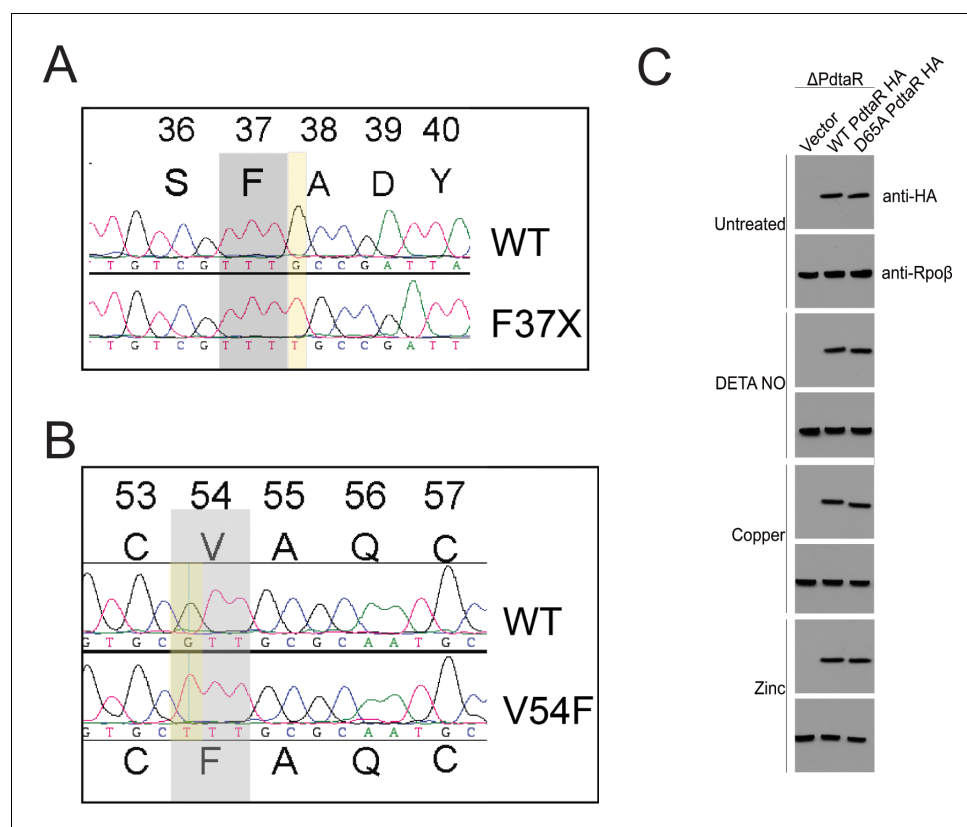


Figure 2—figure supplement 1. Chromosomal PdtaS suppressor mutations and PdtaR levels under stress. (A, B) Chromatograms from sequencing of amplified chromosomal segments from two $\Delta rip1$ suppressor strains with restored Cu resistance. (A) shows the T insertion at amino acid 37 of PdtaS, creating a frameshift mutation. (B) shows a G>T mutation that encodes V54F in PdtaS. (C) Western blotting with anti-HA antibodies in *M. tuberculosis* $\Delta pdtaR$ complemented with vector, WT PdtaR HA, or PdtaR-D65A-HA in the indicated stress conditions.

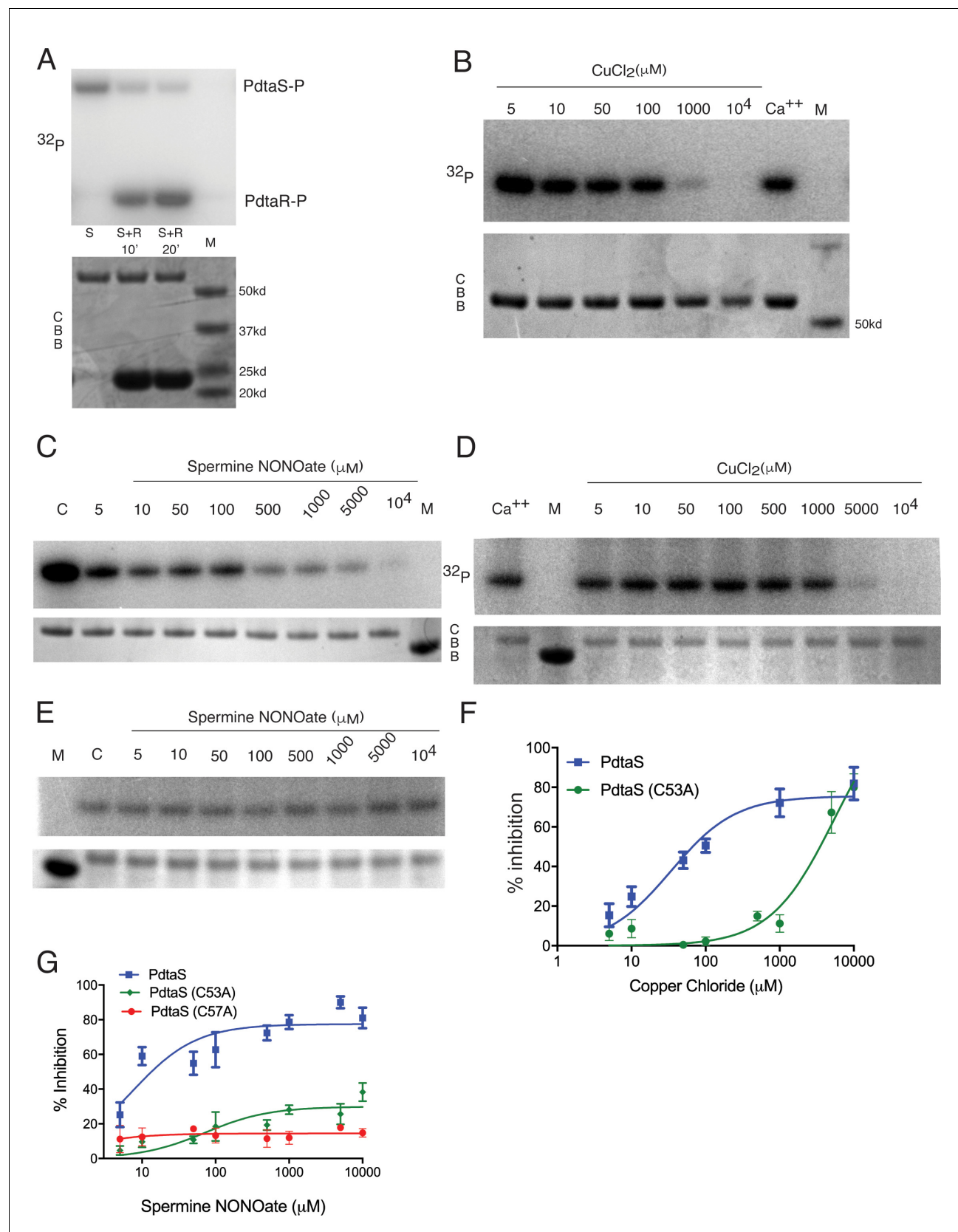


Figure 3. PdtaS is directly inhibited by copper and NO through a dicysteine motif in the N-terminal GAF domain. (A) PdtaS phosphotransfer to PdtaR. Upper panel: phosphorscreen imaging of ³²P incorporation; lower panel: Coomassie brilliant blue (CBB) staining to determine total protein. First Figure 3 continued on next page

Figure 3 continued

reaction contains PdtaS alone, second and third lanes contain PdtaS/PdtaR incubated for 10 and 20 min, respectively. Fourth lane (M) is the molecular weight (MW) marker. (B) Cu^{++} inhibits PdtaS autophosphorylation. Autophosphorylation of PdtaS protein preincubated with increasing concentrations (5 μM to $10^4 \mu\text{M}$) of CuCl_2 or 1 mM of CaCl_2 (Ca^{++}) as a control. Upper panel: phosphorscreen imaging of ^{32}P incorporation; lower panel: CBB staining to determine total protein. (C) NO inhibits PdtaS autophosphorylation. Autophosphorylation of PdtaS protein preincubated with increasing concentrations (5 μM to $10^4 \mu\text{M}$) of spermine NONOate and 1 mM of spermine NONOate post NO release as control (designated by C). (D) PdtaS GAF domain cysteine 53 is required for copper inhibition. PdtaS-C53A protein preincubated with increasing concentrations (5 μM to $10^4 \mu\text{M}$) of CuCl_2 or 1 mM of CaCl_2 was assayed for autophosphorylation as described in panel B. (E) PdtaS GAF domain cysteine 53 is required for NO inhibition. PdtaS-C53A protein preincubated with increasing concentrations (5 μM to $10^4 \mu\text{M}$) of spermine NONOate and of 1 mM of spermine NONOate post NO release as control was followed by autophosphorylation. (F) Cu inhibition curve from replicate data represented by (B) and (D) for PdtaS (blue) and PdtaS-C53A (green) proteins yields K_i of $(34 \pm 8 \mu\text{M})$ for PdtaS and $(5540 \pm 2381 \mu\text{M})$ for PdtaS-C53A. Error bars are SEM for $n = 3$. (G) NO inhibition curve from replicate data represented by (C) and (E) and (Figure 3—figure supplement 2) for PdtaS (blue), PdtaS-C53A (green), or PdtaS-C57A (red) proteins yields K_i of $(7 \pm 2 \mu\text{M})$ for PdtaS and $(73 \pm 34 \mu\text{M})$ for PdtaS-C53A. Error bars are SEM for $n = 3$ for WT and C53A and $n = 2$ for C57A.

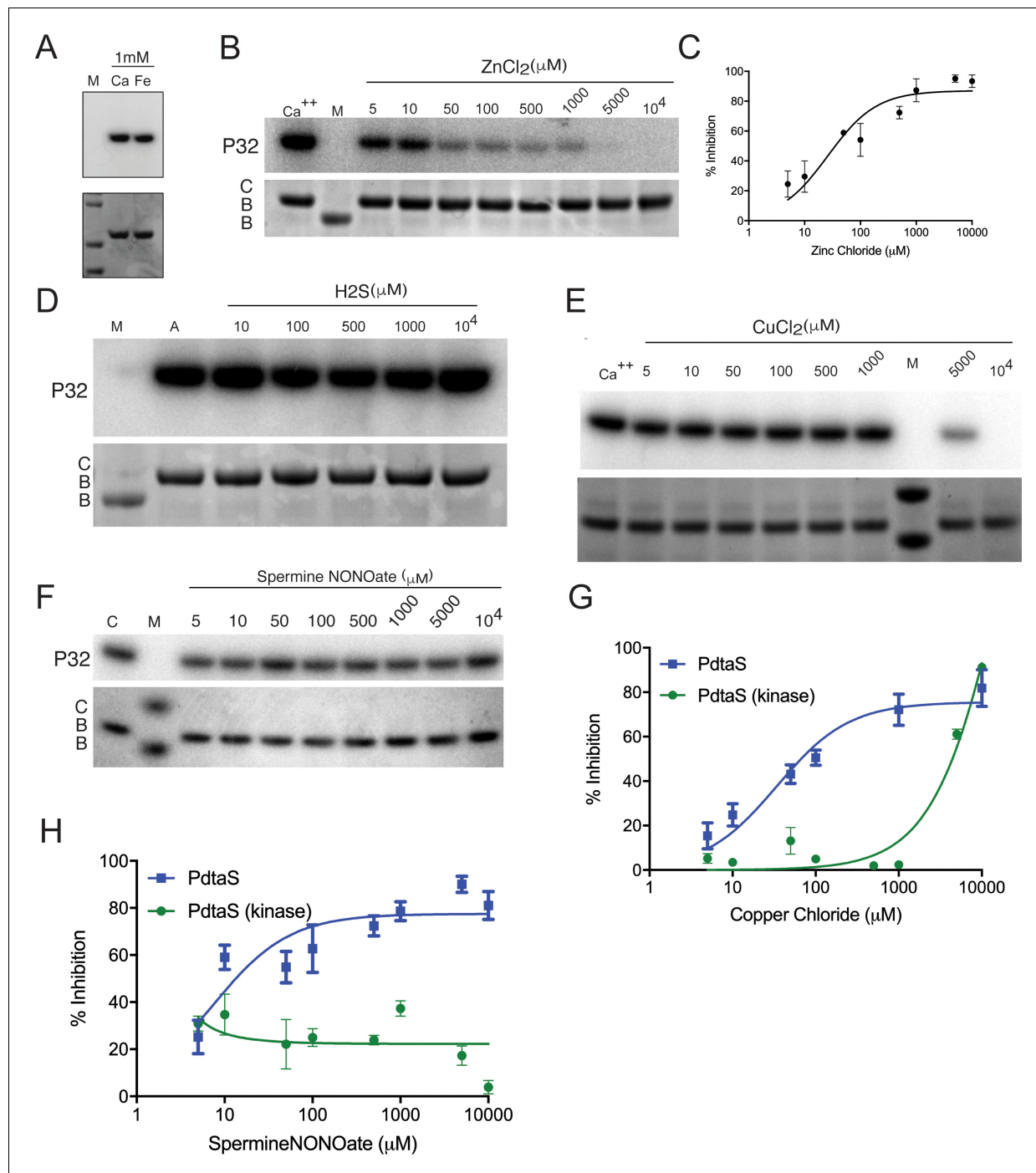


Figure 3—figure supplement 1. PdtaS is inhibited by Zn and Cu through its GAF domain. (A) PdtaS is not inhibited by calcium or iron. Autophosphorylation of PdtaS protein preincubated with 1 mM CaCl₂ or FeCl₂. Upper panel: phosphorscreen imaging of ³²P incorporation; lower panel: Coomassie brilliant blue (CBB) staining to determine total protein. M: molecular weight marker. (B) Zinc inhibits PdtaS autophosphorylation. Autophosphorylation of PdtaS protein preincubated with increasing concentrations (5 μM to 10 mM) of ZnCl₂ or 1 mM of CaCl₂ (Ca⁺⁺) as a control. Upper panel: phosphorscreen imaging of ³²P incorporation; lower panel: CBB staining to determine total protein. (C) Zn inhibition curve from replicate data represented by (B) for PdtaS protein. Error bars are SEM for n = 3. (D) PdtaS is not inhibited by H₂S. Same assay as in (B), but with escalating concentration of H₂S from sodium hydrosulfide hydrate. (E) The PdtaS kinase domain is not inhibited by Cu. PdtaS-kinase (amino acids 277–501) domain was assayed for autophosphorylation with the indicated concentrations of CuCl₂. (F) The PdtaS kinase domain is not inhibited by NO. PdtaS-kinase (amino acids 277–501) domain was assayed for autophosphorylation with the indicated concentrations of spermine NONOate. (G) Cu inhibition curve from replicate data represented by (E) for PdtaS-kinase domain protein. The WT PdtaS curve is the same data presented in **Figure 3F**. Error bars

Figure 3—figure supplement 1 continued on next page

Figure 3—figure supplement 1 continued

are SEM for $n = 3$. (H) NO inhibition curve from replicate data represented by (F) for PdtaS-kinase domain protein. The WT PdtaS curve is the same data presented in **Figure 3G**. Error bars are SEM for $n = 3$.

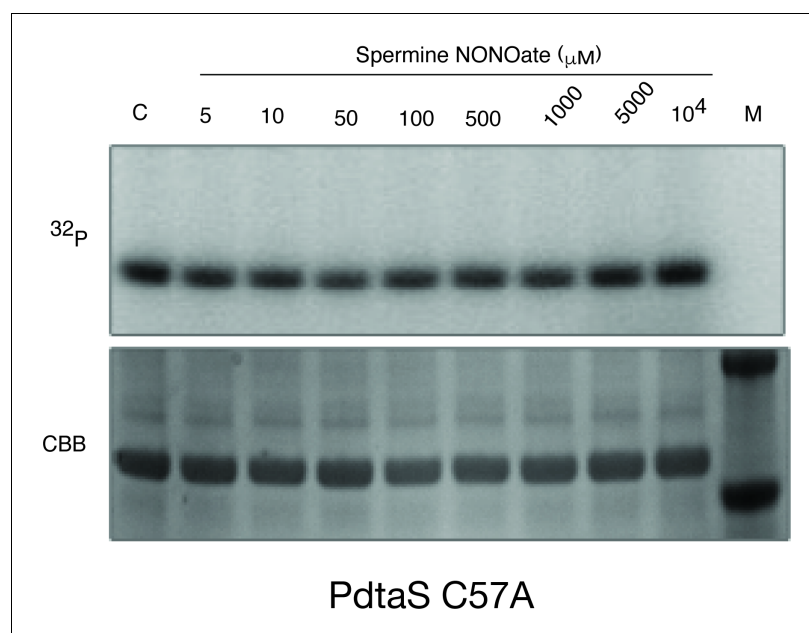


Figure 3—figure supplement 2. PdtaS C57A is not inhibited by NO. Autophosphorylation of the PdtaS protein as in **Figure 3** using the PdtaS-C57A protein.

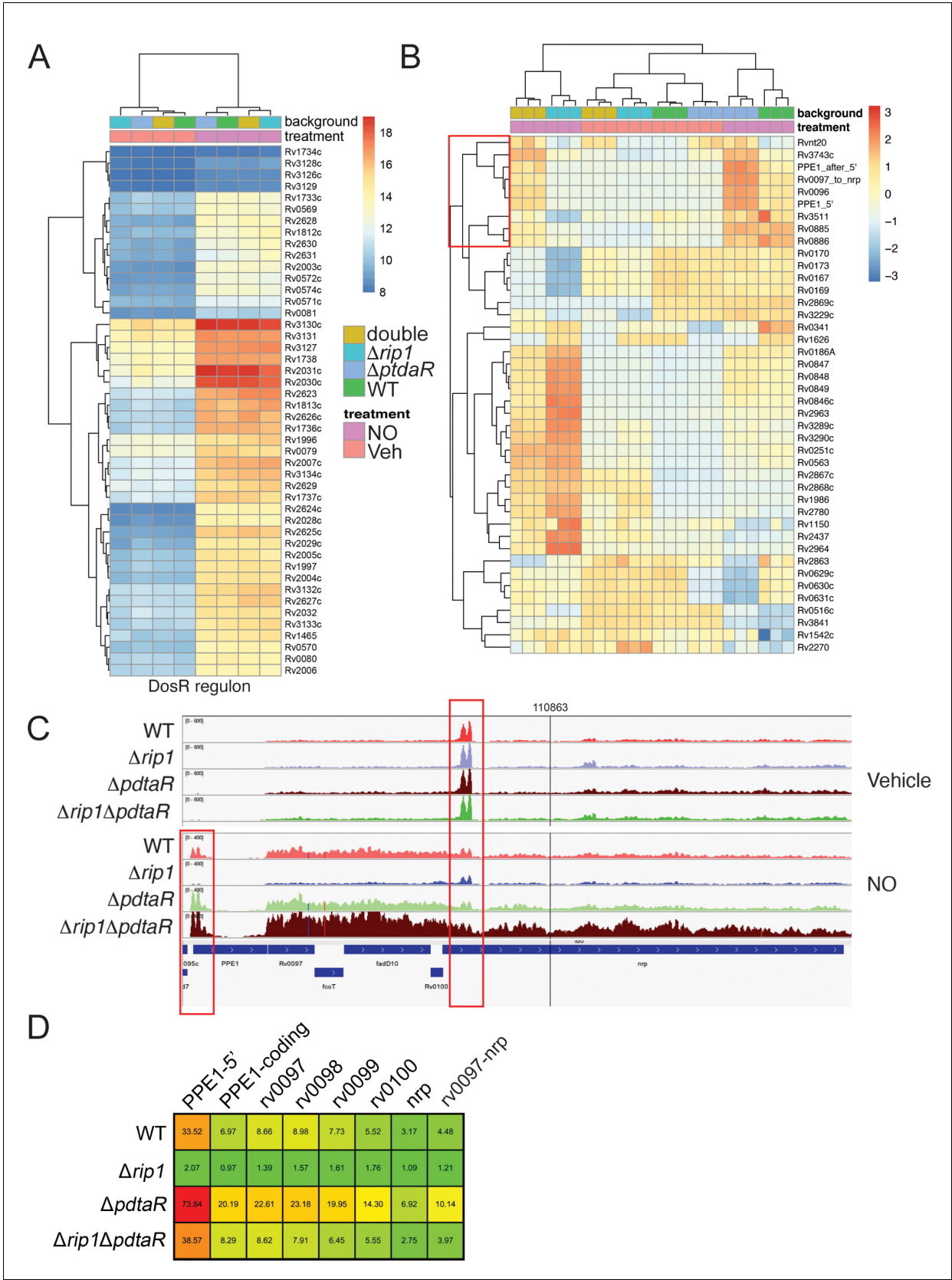


Figure 4. NO-induced dual regulation of the chalkophore biosynthetic operon by Rip1/PdtA/PdtR. (A) Unsupervised clustering of the diethylenetriamine nitric oxide (DETA-NO) (NO)-induced, DosR-regulated transcripts across the indicated genotypes. The scale bar represents the log₂ Figure 4 continued on next page

Figure 4 continued

of the normalized counts for each gene. (B) Unsupervised clustering of gene expression of *M. tuberculosis* WT, $\Delta rip1$, $\Delta pdaR$, and $\Delta rip1\Delta pdaR$ using the same color coding as in (A) treated with vehicle (V) or DETA-NO (NO). The highlighted cluster indicated by the red box on the left includes PPE1-5', the PPE1 coding sequences after PPE1 (PPE1-after 5'), and the *Rv0097-nrp* cluster as independent elements. The scale bar represents the \log_2 of the scaled expression level for each row. The clustering of the genes and strains/conditions is done on the raw normalized counts. (C) Read coverage tracks across the *ppe1-nrp* cluster. Boxed areas highlight *ppe1*-5' peak at the 5' end of PPE1 and a region of potential termination at 5' end of *nrp*. (D) DETA-NO-induced fold change values (DETA-NO/vehicle) across the same coverage region as in (C). *0097-nrp* designates the entire *Rv0097-nrp* cluster.

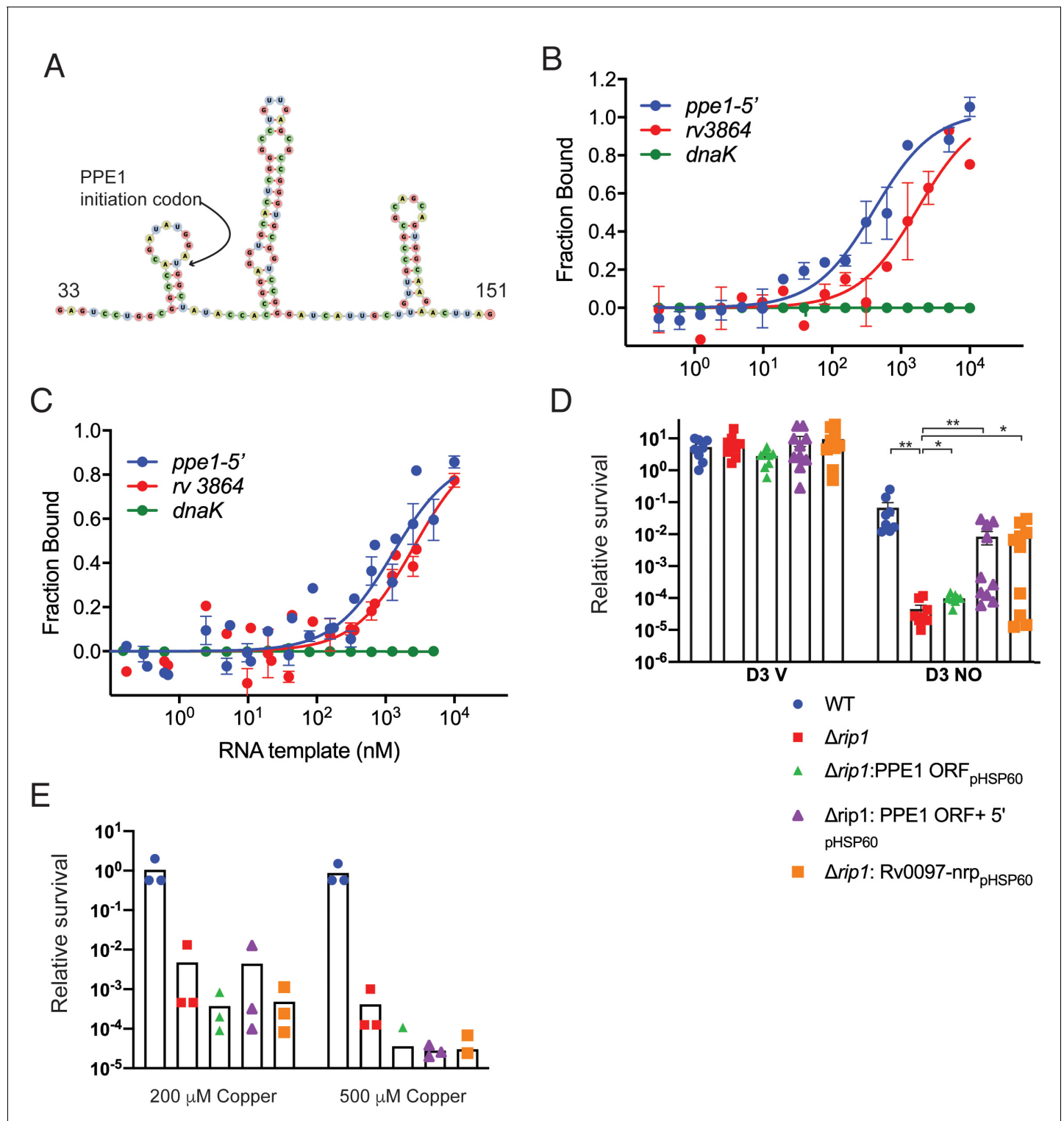


Figure 5. The PPE1-5' RNA is an effector of NO resistance through sequestration of PdaR. (A) Predicted structure of the RNA hairpins in PPE1-5'. The nucleotide numbering refers to distance from the first transcribed nucleotide of the *ppe1* RNA. The PPE1 translational initiation codon is indicated within the first hairpin. (B) Phosphorylated PdaR directly binds to *ppe1-5'*. Change in the thermophoretic movement of fluorescently labeled and phosphorylated PdaR was measured as a function of titrant RNA concentration on the X-axis for *ppe1-5'*, *rv3864*, and *dnaK* (ranging from 0.31 nM to 10 μM) as described in Materials and Methods yielding binding affinity constants (K_d) for *ppe1-5'* = 410 ± 84 nM, *rv3864* = 2117 ± 798 nM while *dnaK* shows no binding. Error bars are SEM for $n = 3$. (C) RNA binding by PdaR is partially phosphorylation dependent. Identical assay as in (B) using PdaR

Figure 5 continued on next page

Figure 5 continued

without phosphorylation by PdtaS. Changes in the thermophoretic movement of fluorescently labeled PdtaR were measured as a function of titrant RNA concentration: *ppe1*-5' (0.15 nM to 10 μ M), *rv3864* (0.61 to 10 μ M), and *dnaK* (0.15 nM to 10 μ M). Binding affinities (K_d) are *ppe1*-5' = 1281 ± 322 nM, *rv3864* = 2592 ± 832 nM while *dnaK* shows no binding. Error bars represent SEM for $n = 3$. (D) Rip1/PdtaS/PdtaR control of PPE1-5' and chalkophore biosynthesis controls NO resistance. Constitutive expression of annotated protein coding region of *ppe1* alone (+*ppe1* ORF *hsp60*), *ppe1* coding region plus 222-nt 5' of start codon (+*ppe1*-5'), both C-terminally fused to GFP, or the chalkophore cluster (+*rv0097-nrp*) in Δ *rip1* and testing for diethylenetriamine nitric oxide (DETA-NO) sensitivity. Relative survival of the indicated strains post treatment with vehicle or 200 μ M DETA-NO. $n = 8$ biological replicates for WT, Δ *rip1*, Δ *rip1*: PPE1 ORF_{pHSP60}; $n = 10$ biological replicates for Δ *rip1*:PPE1 ORF +5'_{pHSP60} and Δ *rip1*: Rv0097-nrp_{pHSP60}. Statistical analysis by Mann–Whitney test. (E) Rip1/PdtaS/PdtaR control of PPE1-5' and chalkophore biosynthesis does not control copper resistance. Relative survival of the same strains as in (D) grown on agar plates supplemented with 0, 200, or 500 μ M copper sulfate normalized as in **Figure 1**. Each value is the average of technical duplicate measurements for $n = 3$ biological replicates. For all panels, statistical significance by t-test analysis is represented as * $p < 0.05$, ** $p < 0.01$, *** $p < 0.001$.

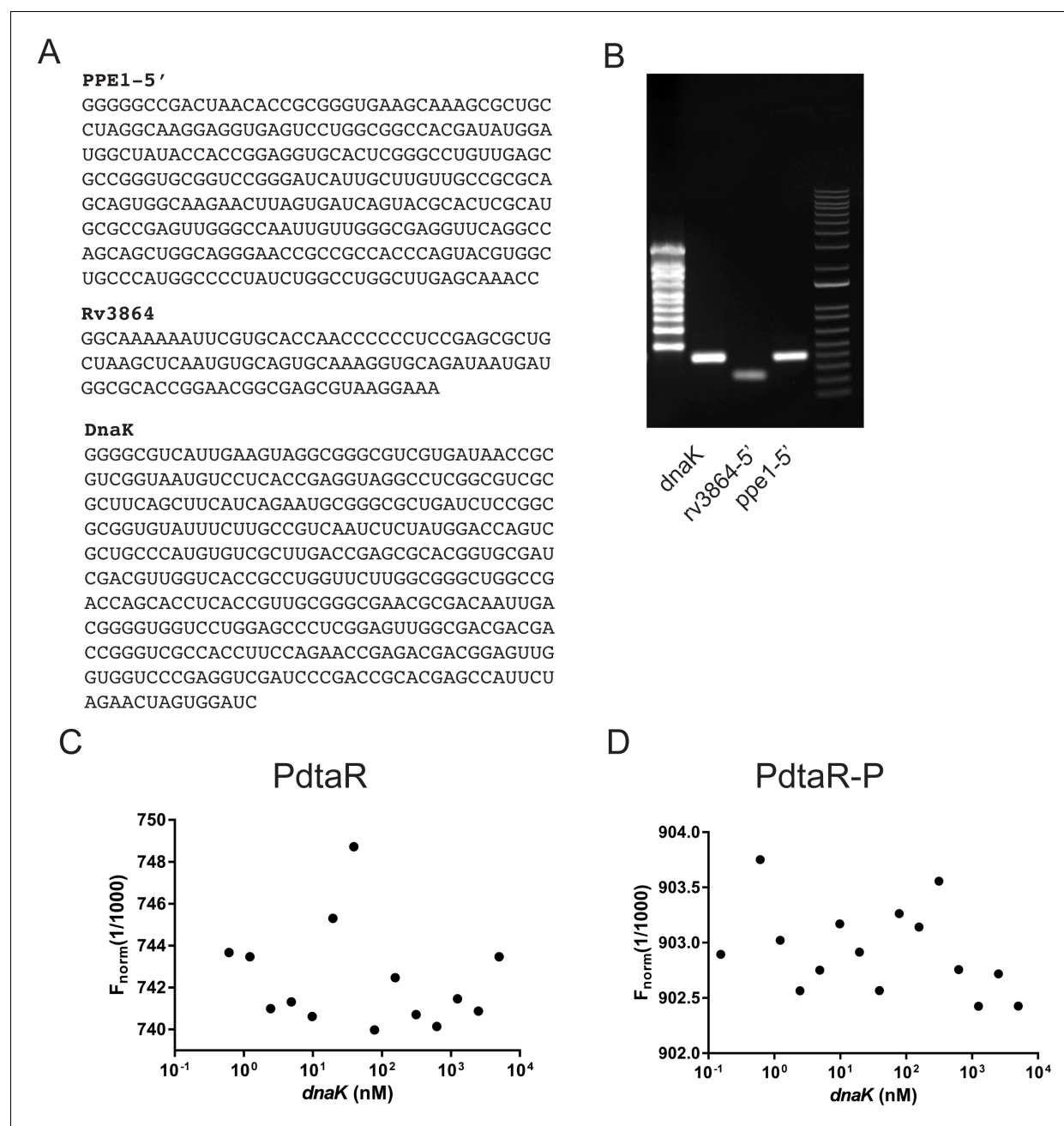


Figure 5—figure supplement 1. RNAs used in PdtaR binding experiments. (A) RNA sequences of RNAs produced by in vitro transcription and used in binding studies in **Figure 5B, C**. (B) Gel electrophoresis of purified RNAs produced by in vitro transcription. (C, D) Microscale thermophoresis titrations for *dnaK* RNA showing no appreciable binding to PdtaR (C) or PdtaR-P (D) for the DnaK RNA. This data is represented on the binding curves in **Figure 5B, C**.

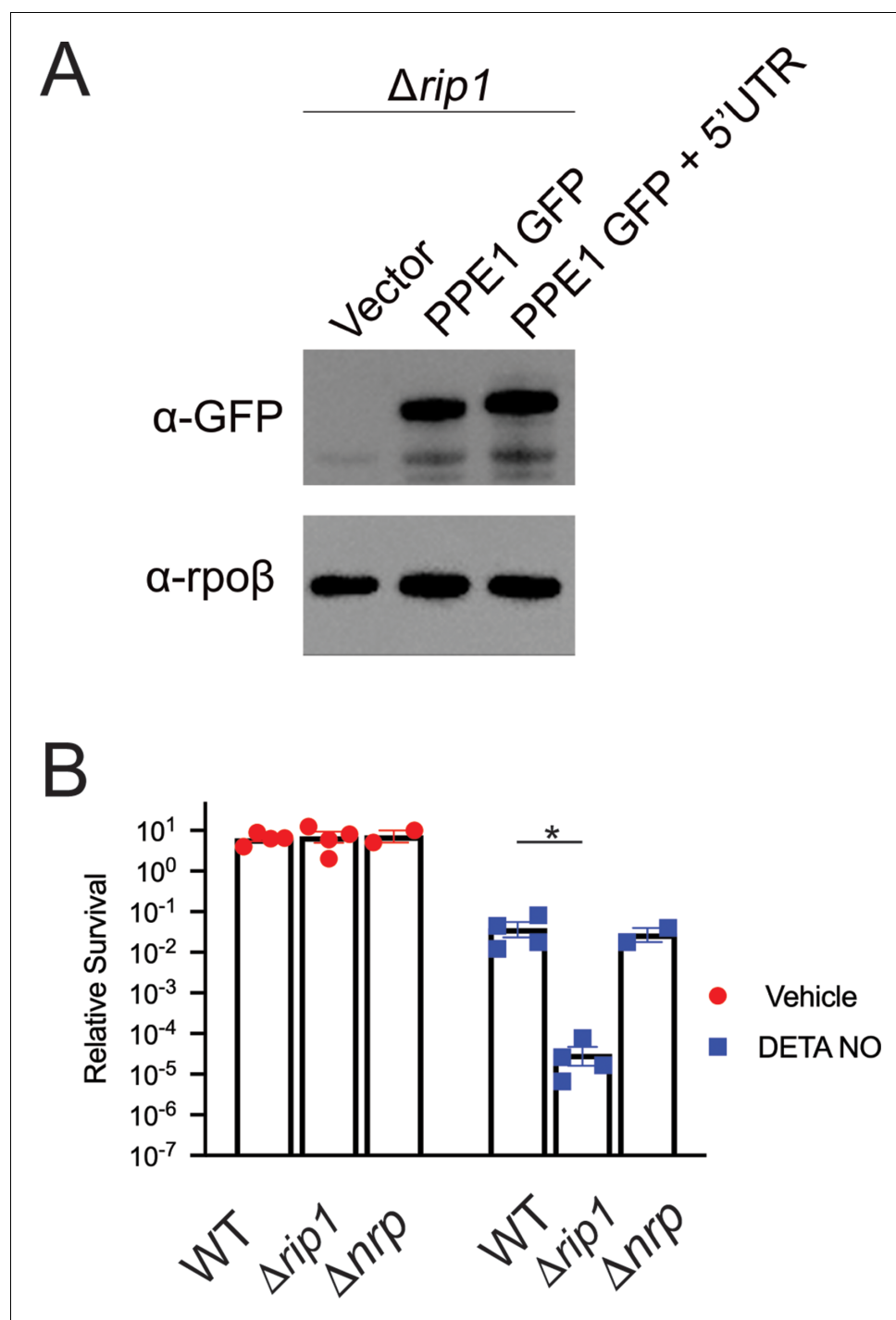


Figure 5—figure supplement 2. PPE1-5' UTR does not affect PPE1 protein expression and *nrp* loss is not sufficient for NO sensitivity. (A) PPE1 is equivalently expressed independent of PPE-5'. *Δrip1* cells transformed with vector, or plasmids encoding C-terminal GFP fused PPE1 ORF (PPE1 GFP), or C-terminal GFP fused PPE1 ORF + PPE1-5' (PPE1 GFP + 5'UTR), both expressed from the *hsp60* promoter, were lysed and blotted as described in Materials and methods. Upper panel: anti-GFP; lower panel: Rpoβ loading control. (B) Loss of chalkophore biosynthesis alone does not confer NO sensitivity. Colony-forming unit (CFU) counts of the indicated strains post treatment with vehicle or 200 μM diethylenetriamine nitric oxide (DETA-NO) for 3 days. Relative survival = CFU day 3 post treatment/CFU at day 0 for each condition. n = 4 biological replicates for WT and *Δrip1*; n = 2 biological replicates for *Δnrp*. *p<0.05 by unpaired t-test.

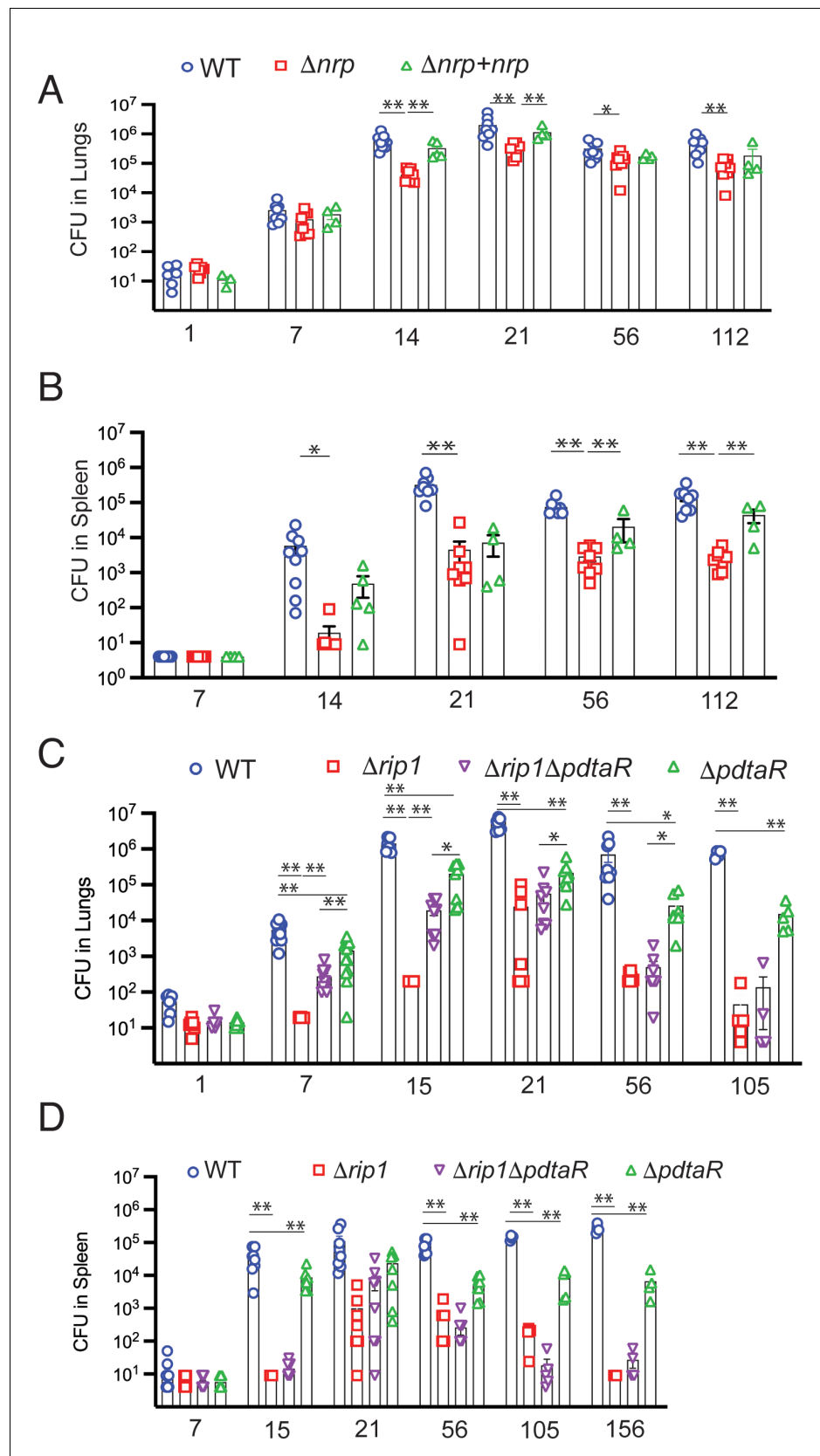


Figure 6. Rip1/PdtaS/PdtaR control of chalkophore biosynthesis controls early lung infection. (A, B) Bacterial burden (colony-forming unit [CFU]) of the indicated strains in lungs (A) or spleens (B) of C57bl/6 mice infected with

Figure 6 continued on next page

Figure 6 continued

WT (blue circle), Δnrp (red square), or $\Delta nrp + nrp$ (green triangle) at the indicated time points (days) post aerosol infection. For WT and Δnrp , $n = 6$ biological replicates on day 1 and $n = 8$ on all subsequent days. All p values calculated by unpaired t -test. (C, D) Bacterial burden (CFU) of the indicated strains in lungs (C) or spleens (D) of C57bl/6 mice infected with WT (blue circle), $\Delta rip1$ (red square), or $\Delta rip1\Delta pdtaR$ (purple inverted triangle) or $\Delta pdtaR$ (green triangle) at the indicated time points (days) post aerosol infection. For all strains, $n = 5$ biological replicates on day 1; $n = 12$ biological replicates on day 7; $n = 8$ biological replicates on days 15, 21, and 56; $n = 4$ biological replicates on days 105 and 156. For all panels, statistical significance by unpaired Welch's t -test is represented as $*p < 0.05$, $**p < 0.01$.

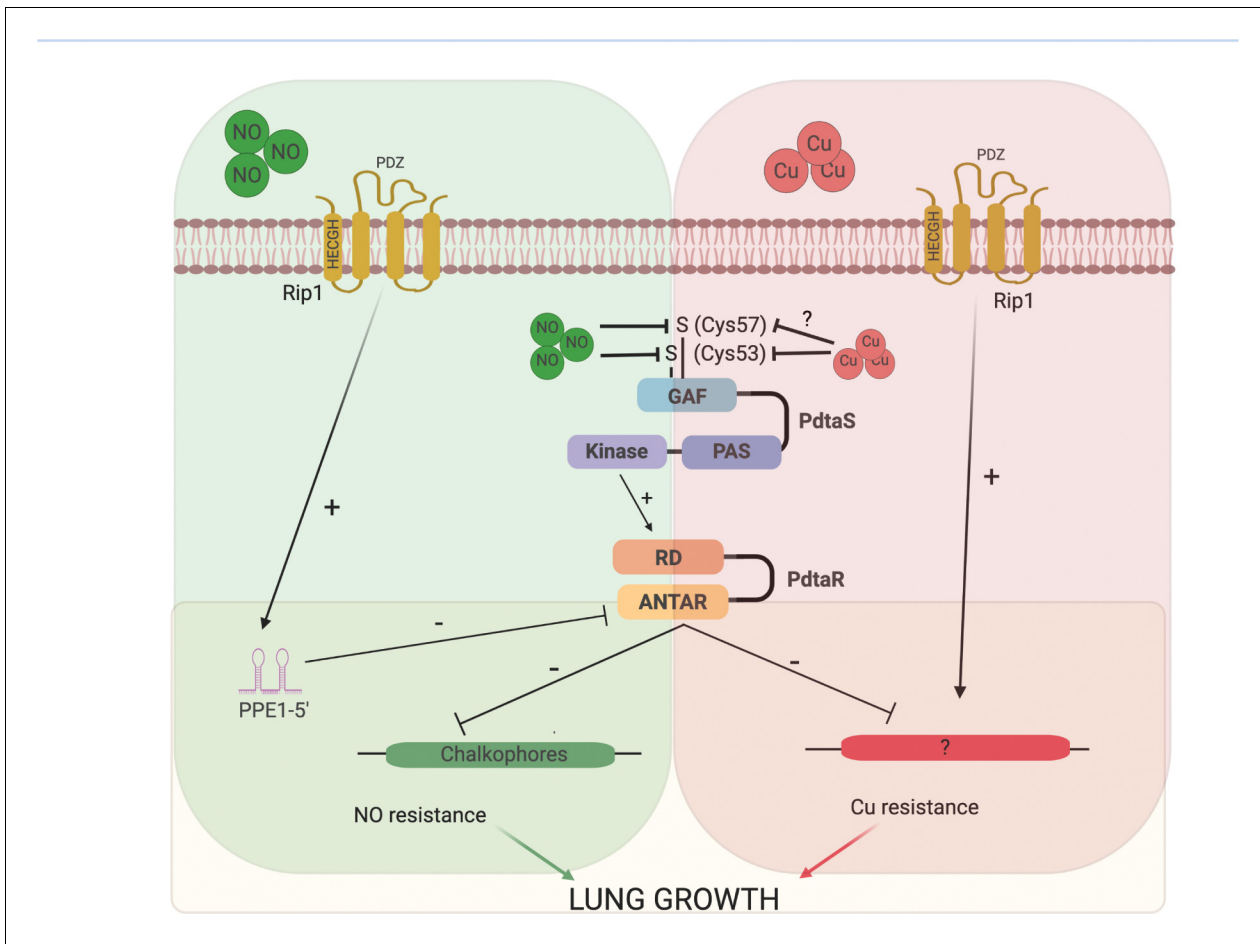


Figure 7. Model of the Rip1/PdtaS/PdtaR signaling circuit and its response to copper and nitric oxide. NO and copper resistance is mediated by cell surface and cytoplasmic convergent signals that inactivate PdtaS/PdtaR. In basal conditions, PdtaS/R is constitutively active, and that activity holds virulence genes, including chalkophore biosynthesis, inactive. NO or copper directly inhibit PdtaS activity through direct sensing by PdtaS N-terminal GAF domain. NO shutoff of PdtaS kinase activity requires C53 and 57, whereas Cu shutoff requires C53 with the role of C57 unknown. Sensing of NO at the cell surface contributes a second signal to relief of PdtaS/R by inducing Rip1-dependent expression of a hairpin containing small RNA at the 5' end of the PPE1 gene (PPE1-5'), which binds directly to the ANTAR domain containing PdtaR. These signals relieve PdtaS/R repression of virulence gene expression, including chalkophore biosynthesis, to activate NO resistance. Although our data clearly implicates the upstream Rip1/PdtaS/PdtaR cascade in Cu resistance, the downstream targets that mediate Cu resistance are not known (indicated by ?). Despite the high Cu affinity of the isonitriles produced by the *nrp* locus, these molecules are involved in the NO resistance arm of the pathway rather than Cu. Figure constructed with BioRender.